AIMS Energy, 3(4): 635-665.
DOI: 10.3934/energy.2015.4.635
Received date 14 April 2015,
Accepted date 14 October 2015,
Published date 19 October 2015

http://www.aimspress.com/

Research article

Coal gasification by indirect heating in a single moving bed reactor: Process development & simulation

Junaid Akhlas [1,3,*], Silvia Baesso [2], Alberto Bertucco [1], and Fabio Ruggeri [2]

[1] Department of Industrial Engineering (DII), University of Padova, via Marzolo 9, Padova, Italy
[2] Amec Foster Wheeler Italiana, via Sebastiano Caboto 1E, Corsico, Milano, Italy
[3] NED University of Engineering & Technology, Karachi, Pakistan

* **Correspondence**: Email: junaid.akhlas@studenti.unipd.it; Tel: +39-324-6293887.

Abstract: In this work, the development and simulation of a new coal gasification process with indirect heat supply is performed. In this way, the need of pure oxygen production as in a conventional gasification process is avoided. The feasibility and energetic self-sufficiency of the proposed processes are addressed. To avoid the need of Air Separation Unit, the heat required by gasification reactions is supplied by the combustion flue gases, and transferred to the reacting mixture through a bayonet heat exchanger installed inside the gasifier. Two alternatives for the flue gas generation have been investigated and compared. The proposed processes are modeled using chemical kinetics validated on experimental gasification data by means of a standard process simulator (Aspen Plus™), integrated with a spreadsheet for the modeling of a special type of heat exchanger. Simulation results are presented and discussed for proposed integrated process schemes. It is shown that they do not need external energy supply and ensure overall efficiencies comparable to conventional processes while producing syngas with lower content of carbon dioxide.

Keywords: indirect gasification; bayonet heat exchanger; syngas from bituminous coal; process simulation; heat integration

1. Introduction

With the growing world energy requirements and depleting oil and natural gas reserves, the rate of current advancement in the economic optimization of renewable resources stresses upon the reliance on a sustainable utilization of coal reserves for over several decades to come [1]. Coal gasification is one of the processes developed for the purpose of using coal in a way that the environment contaminant emissions from the process are minimized as compared to the direct use of burning coal as fuel, which causes at least 70% of anthropogenous CO_2 emissions of Europe [2]. Furthermore, this process helps in increasing the possibility of utilizing largely abundant coal reserves of both high and low quality [3] to provide gaseous fuel to compensate for and reduce the use of constantly and rapidly diminishing natural gas reserves. The Syngas produced can be used for a wide variety of downstream processes such as for power generation (IGCC), the production of refinery utilities (H_2, steam, power), chemical synthesis (methanol, ammonia, oxochemicals), methanation and liquid fuels production.

The objective of this work is to simulate and determine the energy efficiency of an original coal gasification process which uses steam instead of air or oxygen. Coal Gasification can be carried out with air, oxygen, steam, or a combination of them. Using air has the disadvantage of lower product gas quality as nitrogen in the air dilutes it. On the other hand, using pure oxygen or oxygen rich air, a higher quality syngas can be obtained but this leads to the heavy generator power consumption associated with the use of an air separation unit [4,5,6] with an overall impact of 5–7% on gross power generator output [7]. Therefore, in the proposed schemes, the impacts of air or oxygen as the oxidant to provide gasification heat are avoided by using steam as the sole gasifying medium.

A counter-current moving bed gasifier with high-pressure superheated steam injection at the bottom is considered. The counter-current scheme is chosen to avoid the inhibition of the gasification reaction caused by the presence of pyrolysis gases in the gasification zone. Bayarsaikhan et al. [8] observed that the pyrolysis gases created in a fluidized bed gasifier limit the char conversion in steam to a range of 62–85%. In the proposed gasifier, ash along with unreacted char is withdrawn at the bottom and the raw syngas mixed with unconverted steam is obtained at the top of the gasifier.

In the absence of oxygen or air, the heat of reaction is provided by the flue gases which are generated through the external combustion of fuel already available in the process. Two alternatives have been investigated for flue gas generation: 1) the coal conversion is maximized in the gasifier, and part of the syngas produced is then burnt in a furnace; and 2) only partial conversion of coal is achieved in the gasifier, and the unconverted char is fed to the furnace downstream. The heat exchange between the flue gases and the gasifier environment is carried out through an annular type of heat exchanger i.e. bank of bayonet tubes vertically installed within the reactor.

In this study, Aspen Plus™ is utilized to simulate process kinetics and overall process heat integration while MS Excel™ is used to calculate the indirect heat transfer from the bayonets to the gasification reactor. To estimate and optimize the existing and novel gasification processes, several model based studies have been carried out previously. Wen et al. [9] developed a mechanistic computer model to simulate their experimental work performed earlier [5] on the gasification of bituminous coal in a Lurgi gasifier with steam and oxygen as the gasifying media. But mechanistic models use complex systems of equations to describe a gasification process in terms of chemical

kinetics, physical properties and flow dynamics. In order to avoid extensive efforts required by these numerical models in providing a substantial amount of data, readily available process simulation software can be efficiently used. Several works have been performed to simulate actual gasification processes either in agreement with some experimental data or to provide a forecast of sufficient thermodynamic advantage of a newly proposed gasification scheme. Aspen Plus™ has been used for various types of gasification processes by several authors such as Sudiro et al. [10,11] and Zhang et al. [12] for dual bed gasification processes and more recently Arthur et al. [13] for a transport gasifier. Feng et al. [14] proposed a steady-state kinetic model in Aspen Plus™ for a pressurized fixed bed Lurgi gasifier of industrial scale to investigate the sensitivity of the scheme towards variations in mass ratios of oxygen and steam to coal feed, which again provides a process simulation model for an oxygen and steam fed gasifier but for a highly volatile lignite coal. Some studies are carried out to investigate novel indirect gasification methods other than dual bed configuration. Kawabata et al. [15] have studied the effects of exergy recuperation in a triple-bed combined circulating fluidized bed gasifier where steam is the sole gasification medium while the reaction heat is provided by the exhaust gases of a high temperature gas turbine. Duan et al. [16] have thermodynamically studied the production of hydrogen rich gas from the steam gasification of coal using blast furnace slag as the heat carrier.

Our work though focuses on determining the performance of an industrial scale, single moving bed gasifier fed with bituminous coal with steam as the single gasification agent. The coal used for this simulation analysis is Pittsburgh No. 8, which was considered for syngas production in a Lurgi gasifier by Wen et al. [5]. The scope of this work is focused on proposing and testing a new gasification process, on the basis of energy efficiency analyses. Economic evaluation of the proposed schemes is not carried out at this stage.

2. Development of Process Scheme

The reactor developed and simulated in this work is shown in Figure 1. It is a moving bed type coal gasification reactor where the coal is fed from the top hopper, with high pressure super-heated steam as the gasifying medium, entering the lower part of the reactor. The heat of the endothermic gasification reaction is provided by the vertical bayonet tube heat exchangers installed in the reactor. The product gas obtained from the reaction contains CO, H_2, CO_2, CH_4, and the unreacted steam with traces of N_2, H_2S, and tar. The ash is retrieved at the bottom along with unreacted coal. This configuration is chosen to compare the output of this work to the previously reported results for bituminous coal oxygen-steam gasification in a similar gasifier.

The bayonet heat exchanger is comprised of two concentric tubes, in which the fluid enters through the central one. The advantage of this type of layout lies in the possibility of using high-temperature heating streams (flue gases up to 1400 °C), provided that the bayonets are realized with suitable materials resistant to high temperatures [17]. A further characteristic of this type of exchangers is the ability of the two concentric tubes to thermally expand independently from each other, thus making them suitable in environments with high temperature differences [18].

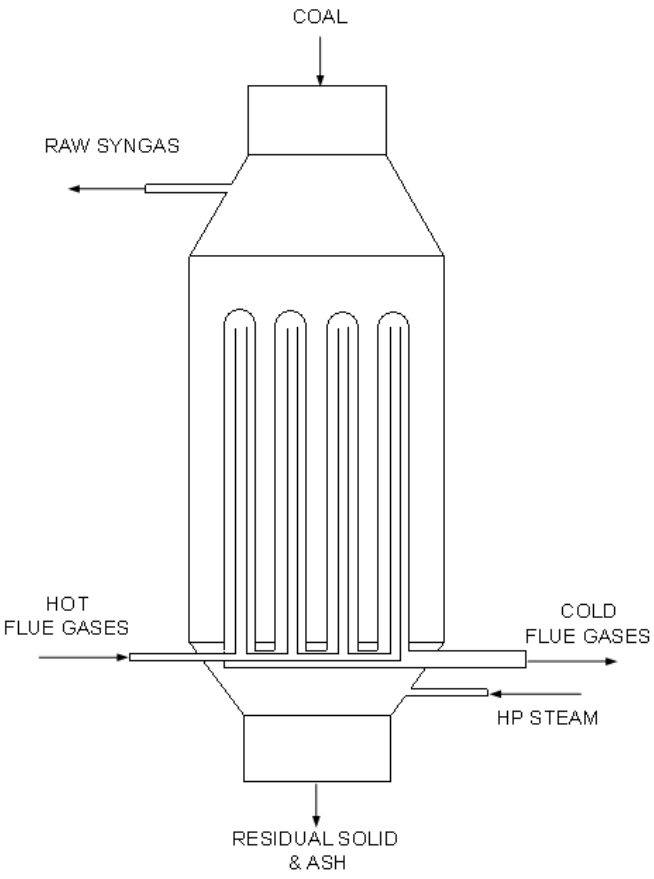

Figure 1. Schematic of the proposed gasifier with indirect heat transfer through a bayonet.

In the topmost section of the gasifier, adiabatic processes of coal drying and coal pyrolysis take place. The drying process removes the physically bound moisture from coal while the pyrolysis process comprises of the removal of volatiles producing a gaseous mixture of permanent gases, light hydrocarbons and tars. The heat for these processes is supplied by the hot gaseous mixture (raw syngas) rising from the rest of gasifier volume below. It is assumed that there is no temperature gradient across the solid and gaseous material streams (char, moisture, pyrolysis gases and raw syngas) in the radial direction. From the results obtained by Hobbs et al. [19], it is known that the length of coal drying and coal pyrolysis sections is comparatively much smaller than the total gasifier length required for gasification. Therefore, it is further assumed that these processes take place as soon as the coal comes in contact with exiting hot gases.

Two schemes are proposed to explore the possibility of the use of post-combustion flue gases as a thermal vector in a bayonet heat exchanger. In first scheme, according to the process Scheme 1, the hot flue gases flowing inside the bayonets are obtained by the combustion of a part of the produced raw syngas in a furnace. The other alternative, shown in Scheme 2, generates the flue gases for heat transfer from the combustion of carbonaceous solid residue out of the gasifier. In both cases, the base for calculation is a coal feed of 70,000 kg/h (19.44 kg/s). In the following sections, the two schemes are explained in detail and some relevant values of process streams variables from the mass and energy balances are reported for better understanding of the process.

2.1. Partial Syngas Combustion Process:

In Scheme 1, the raw syngas produced in the gasifier is split in two streams in a way that temperature of the flue gases downstream can be maintained as required. 55.53% of the raw syngas stream is taken out as the product. The remaining syngas is combusted in the furnace with 20% excess air, to generate 63.89 kg/s of high pressure steam keeping the temperature of hot flue gases at 1300 °C. These gases then provide the heat required for gasification, preheat the air supplied to the furnace, and convert part of feed water into saturated steam. 5.96 kg/s of surplus high pressure saturated steam is generated from the still-hot flue gases before they are finally exhausted at 150 °C. A secondary stream of feed water is converted to saturated steam by cooling the hot product gas from the gasifier down to 180 °C. An adiabatic gasification volume is assumed at the top of the gasifier to use the heat content of the high temperature product gas to help in drying, pyrolysis and partial gasification of the incoming fresh coal. Note that the bayonet inlet temperature of the flue gases produced from the combustion of hot syngas in the furnace is 1300 °C. In such conditions, the central tubes of the bayonets, which are exposed to the high temperature flue gases at inlet, must be made with a suitable material (Appendix C).

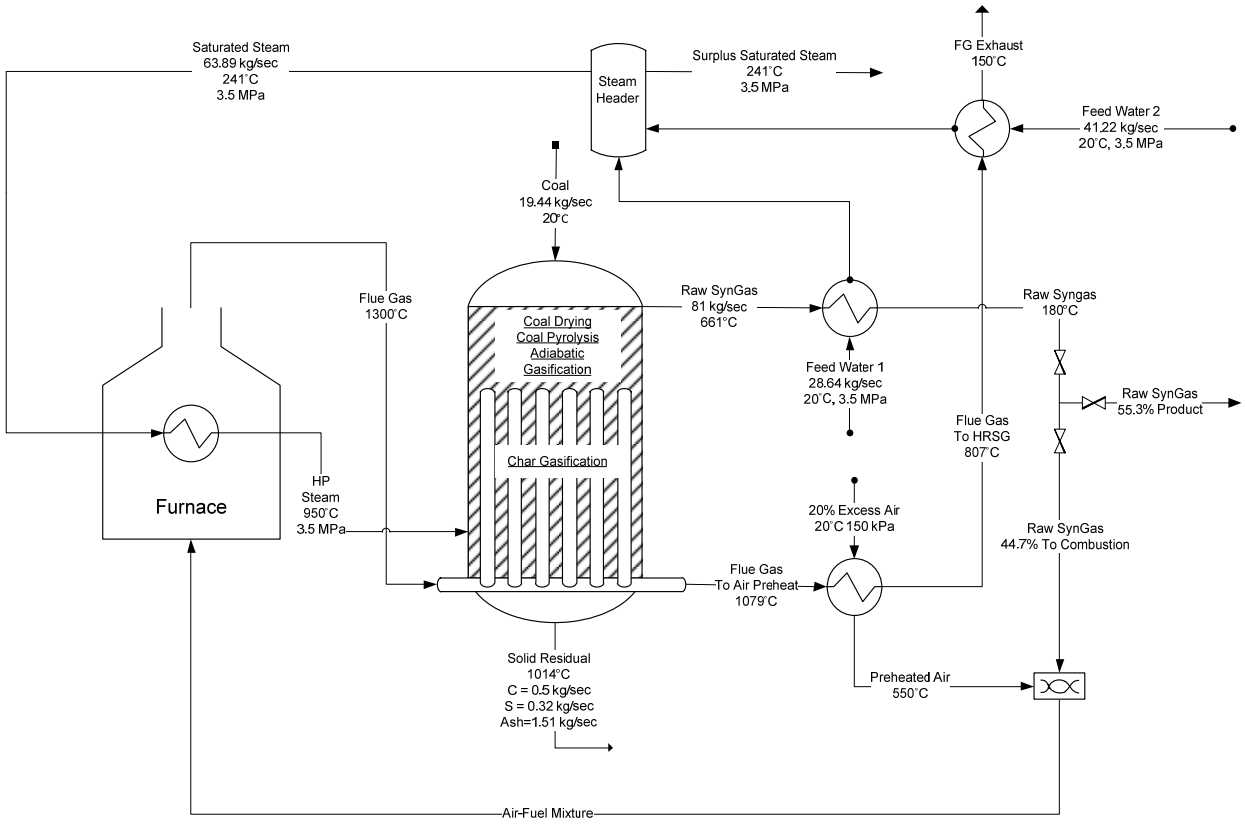

Scheme 1. Simplified process scheme of indirect gasification using the flue gases from the partial product gas combustion as the heat source.

In the upcoming hydrogen and power co-generation schemes, syngas produced is used for the production of hydrogen or other synthetic fuels in a once-through reactor and the unconverted gas is used for power generation after the combustion of syngas in a furnace [20,21]. But, power generated

in this case has also to serve for the ASU. In our Scheme 1, similarly, part of the syngas is "wasted" in combustion and is not available for downstream chemical syntheses. However, it not only provides for the heat of gasification reaction, but generates process steam, preheats combustion air, and provides ample surplus steam for power generation as well.

2.2. Unreacted Char Combustion Process

According to Scheme 2, the flue gases are generated by the combustion of unreacted char flowing out from the gasifier with 30% excess air. The temperature of the flue gases coming out from the furnace burning this char is limited to 1000 °C to avoid ash sintering [22]. This temperature is maintained by producing 38.89 kg/s of high pressure steam at 850 °C and about 35.36 kg/s of surplus high pressure saturated steam at 241 °C. The lower temperature of the flue gases entering the bayonet forces the gasification to be carried out at lower temperature as compared to Scheme 1, limiting the overall carbon conversion to 33.13%. In addition, an adiabatic gasification volume is assumed at the bottom of the gasifier to exploit the heat content of the incoming steam. This starts the steam reforming process and reduces the temperature of the gasification environment, thus increasing the amount of heat that can be drained from the following bayonet section.

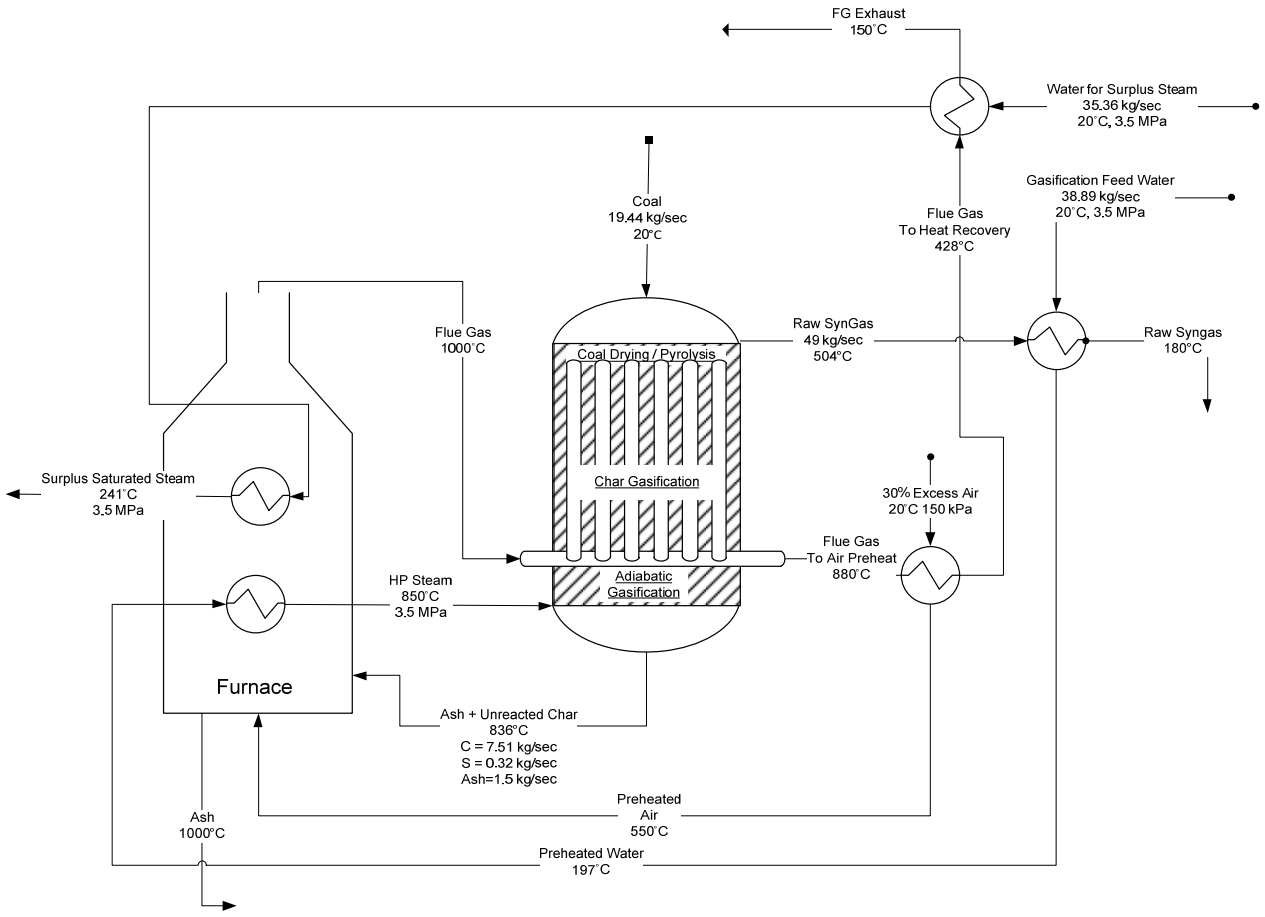

Scheme 2. Simplified process scheme of indirect gasification heated by flue gases from the residual unreacted char combustion.

After exiting from the bayonets, the flue gases then preheat the air supplied to the furnace, and are finally exhausted after heating the water for surplus steam generation. The heat content of the raw hot syngas is utilized to preheat the feed water for gasification before it is superheated in the furnace. These two combinations of hot and cold streams for heat exchange are interchangeable but the net heat utilization effect remains same.

3. Process Modeling

The Process Model for the reaction being carried out with the gasifier reactor is developed in the Aspen Plus™ Process Simulator. The components in the simulation are modeled using Aspen Plus™ guidelines to calculate thermodynamic and transport properties. The conventional components considered for simulation are hydrogen, oxygen, nitrogen, water, methane, carbon monoxide, carbon dioxide, hydrogen sulfide and benzene (to represent tars) in MIXED sub-stream. Carbon and sulfur are modeled in CISOLID sub-stream. To calculate the physical properties of mixed conventional components and of solid components, the property model RKS-BM is used. A non-conventional component sub-stream is also introduced to represent coal, dry coal, char and ash. These are described by defining their component attributes i.e. their Proximate, Ultimate, and Sulfur Analyses. Component attributes of dry coal and char are calculated from the analysis data of original coal and the amount of gaseous pyrolysis products in terms of mass balance. DCOALIGT and HCOALGEN are used to calculate the densities and enthalpies of non-conventional components respectively.

The following assumptions were taken into account while developing the model:

- The process is at steady state;
- Pressure losses are neglected;
- The temperatures of the solid phase and gas phase are equal at any point.

3.1. Gasifier Stages

In the gasifier, three major stages are observable, in sequence: coal drying, coal pyrolysis, and char gasification. As stated earlier, drying and pyrolysis processes take place at the uppermost layer of the gasifier coal bed, therefore relatively simpler modeling approaches have been considered for these stages, whereas detailed modeling has been performed on the gasification section only.

In Coal Drying, the moisture physically bound in the coal is released into the gas phase by taking heat from the incoming hot streams passing through the top portion of the gasifier. The amount of water vaporized is determined from the proximate analysis of the coal i.e. 4.58% of coal fed. The drying section is modeled as a RYield reactor at a temperature of 300 °C [23].

In Coal Pyrolysis, the dried coal is broken down into Char and other gases generated from the conversion of volatile materials into CO, H_2, CO_2, H_2O, H_2S, N_2, CH_4, and tar (represented by C_6H_6), according to:

$$\text{Coal} \rightarrow CO + H_2 + CO_2 + H_2O + H_2S + N_2 + CH_4 + C_6H_6 + \text{Char} \quad (1)$$

The pyrolysis gas becomes part of the product gas stream, while the char goes down into the gasification section. The amount of each pyrolysis product is predicted using the experimental data by Suuberg et al. [24] according to the coal feed ultimate analysis. The results are shown in Table 1. The high amount of char fraction is due to the type of coal utilized. These pyrolysis yields are used as input in a RYield reactor according to Reaction (1). The temperature of pyrolysis is set at 600 °C, according to Zhang et al. [12].

Table 1. Yield of Pyrolysis Products [23].

Components	Yield (mass basis on dried coal, %)
CO	1.9
CO_2	2.25
H_2O	0.65
CH_4	13.95
H_2	0.54
tar	5.79
H_2S	0.94
N_2	0.35
Char	73.63

In order to model the axial mixing within the gasifier, a series of 12 equal volume RCSTR blocks has been applied. The adiabatic sections have been simulated by RCSTR blocks as well. The number of RCSTRs chosen is typical of a flow pattern close to a plug flow reactor. The temperature in each RCSTR is coupled with a corresponding section of the bayonet heat exchanger, whose length is also divided in 12 equal cells (further details in section 3.2). The pressure of each block is 3.5 MPa with a bed voidage linearly varying from 0.4 to 0.7 [23].

To model the kinetics of char gasification, the following reactions are considered [9,25]:

$$C + \frac{Z+2}{2Z+2} O_2 \rightarrow \frac{Z}{Z+1} CO + \frac{1}{Z+1} CO_2 \quad (2)$$

$$C + H_2O \rightarrow CO + H_2 \quad (3)$$

$$C + CO_2 \rightarrow 2CO \quad (4)$$

$$C + 2H_2 \rightarrow CH_4 \quad (5)$$

$$CO + H_2O \rightarrow CO_2 + H_2 \quad (6)$$

$$H_2 + 0.5O_2 \rightarrow H_2O \quad (7)$$

where,

$$Z = \frac{C_{CO}}{C_{CO_2}} = 2500e^{\frac{-6249}{T}} \text{ , [26]} \quad (8)$$

C_{CO} =Mean concentration of CO, kmol/m^3.

C_{CO_2}=Mean concentration of CO_2, kmol/m^3.

T=Temperature, K.

The reactions defined above are of mainly two categories; gas-solid ((2)–(5)) and gas-gas ((6)–(7)). In the gas-solid reaction (2), the rate of reaction is usually fast relative to diffusion rate of oxygen into the coal; therefore this reaction is considered as a surface reaction. Reactions (3)–(5) have rather slow rates of reactions at gasifier temperatures below 1000°C, thus they are volumetric in nature.

In the Aspen Simulation, the reaction kinetics are calculated using an external FORTRAN subroutine, according to the rate equations summarized in Appendix A.

3.2. Heat Transfer Modeling: Bayonet Construction and Set-up

The heat transfer model for the bayonet heat exchanger is based on the one developed by Bussman et al. [27] for variable test furnace cooling in process industries.

Bayonets are special heat exchange devices comprising of two sections. Hot Flue gases from the furnace enter the inner tube of the bayonet and rise to the end of the inner section. At this point, they turn back, and enter the annular section of the bayonet tube, flow back downwards and then discharge from the tube to the circuit downstream. These tubes are installed vertically on the reactor floor. The flow of the flue gases through a simplified diagram of a bayonet tube heat exchanger is shown in Figure 2, together with relevant variables defined in Appendix B.

In the partial product gas combustion process (Scheme 1), the inner tube material is considered to be sintered α-SiC ceramic material to withstand the flue gases entering the bayonet tubes at 1300 °C, while in the residual char combustion Scheme 2, it is of HK-40 heat resistant alloy. The rest of the bayonet assembly (annular section) is considered to be made of HK-40 heat resistant alloy for efficient heat transfer to the mixture of steam & raw syngas in the reactor environment around these bayonet tubes.

The height of each bayonet tube is 18 m to allow the required heat transfer to the gasification reaction. The ceramic portion of the tube may be assembled in parts (for ease in fabrication) as no absolute sealing is mandatory between the flue gases in central and annular sections of the bayonet which are assumed to be at same pressure. To facilitate the calculations and profiling of the heat transfer and temperature distribution along the length of the bayonet tubes, these are divided in 12 hypothetical cells of length 1.50 m each. As 5 meters more are needed to account for the adiabatic region of gasification, the total reactor height is 23 m.

Following assumptions were taken into account while developing the calculation model for the heat transfer through the bayonet tubes to the reactor.

1. Thermal properties of the gaseous streams (flue gases flowing inside the central and annular sections of the bayonet and gasifier gases flowing externally over the annular section) vary

from top to bottom with temperature and composition fluctuations. Therefore, the division of the bayonet length in 12 cells helps in taking into account this variation and thus these thermal properties are calculated at the mean temperature of each cell.

2. Radial heat transfer supersedes the axial heat transfer through the bayonet walls.
3. Outer annular surface of each cell is assumed to be surrounded by a thin layer of gases flowing in the gasifier from bottom to top along the length of the bayonet tube heat-exchanger.
4. Heat transfer by radiation is considered to take place from the center pipe wall to the annulus inner wall and from the annulus outer wall to the reactor volume.
5. The heat exchange at the top hemispherical section of the bayonet tubes is neglected as the hemispherical area at the top (0.016 m^2) is 30 times smaller than the area of one cell (0.471 m^2) i.e. 360^{th} part of the entire bayonet.

Table 2 summarizes the dimensions of the reactor, the bayonet tubes and their distribution in the gasifier cross section [28]. The coal is assumed to flow only between two adjacent rows of bayonet tubes.

Appendix B summarizes the energy balances and material properties utilized in calculating the heat transferred to the gasification reaction through the length of the bayonet tubes. This model is formulated in an Excel™ spreadsheet.

Table 2. Dimensions of the gasifier reactor.

REACTOR VESSEL	Diameter [7]	5.0 m
BAYONETS	Number of Bayonets (Linear Pitch)	487
	Number of rows	15
	External tube outer radius	5.0 cm
	Internal tube outer radius	3.8 cm
	Tubes' thickness	0.5 cm
	Distance between two consecutive bayonets in a tube row	1.0 cm
	Distance between two consecutive tube rows	22 cm
	Minimum Clearance between wall and the tube bank	22 cm

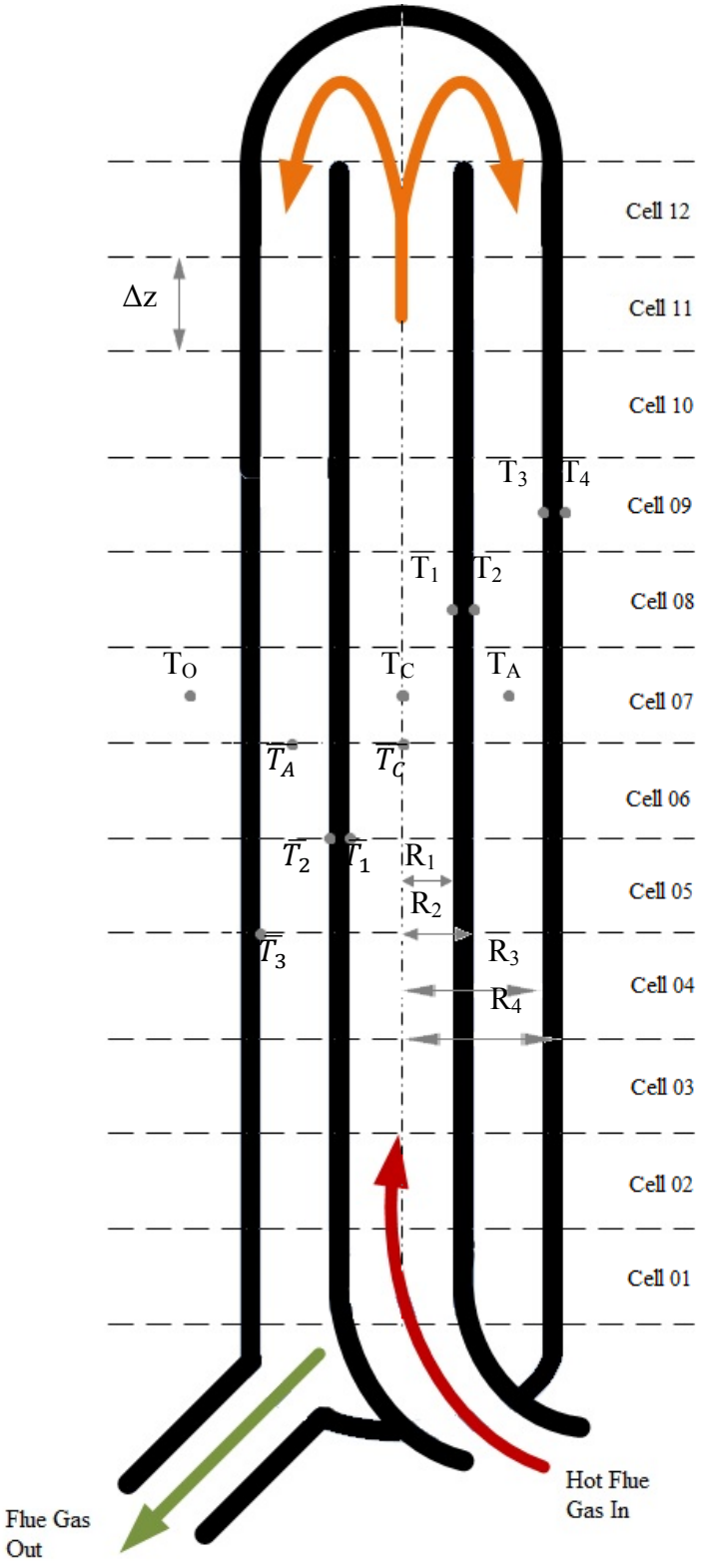

Figure 2. Schematic of a bayonet tube heat exchanger (Refer to Appendix B).

4. Process Simulation

4.1. Input Parameters

Simulation input parameters are defined in Table 3.

Table 3. Input Parameters for the gasification simulation.

Combustion Mode	Partial Product Gas	Unreacted Char	Reference/ Basis
Gasification Pressure (MPa)	3.5	3.5	[23]
Steam flow rate in (kg/s)	63.89	38.89	Preliminary Sensitivity Analysis
Steam/Coal Ratio (kg/kg)	3.3	2.0	
Steam-in Temperature (°C)	950	850	
Excess Air in Furnace (%)	20	30	
Air Pre-heat Temperature (°C)	550	550	
Flue gas temperature at bayonet inlet (°C)	1300	1000	Furnace Fuel Type

Preliminary sensitivity analyses were performed (not reported) in order to determine some of the values stated above. Steam input flowrate (and thus the steam to coal ratio) and temperature are chosen in order to keep the maximum gasification temperature below 1050 °C. In the unreacted char combustion scheme, there is a lower steam input because of a lower coal conversion to be achieved in the gasifier; while the steam temperature is limited to 850 °C by the temperature limitation in the residual coal furnace. Combustion air excess varies between the two schemes because of the fuel nature (solid and gaseous) providing the optimum flowrate of flue gases inside the bayonet tubes to supply the required heat transfer. Air pre-heat temperature is set based on the known industrial practices. In the case of partial product gas combustion, absence of ash sintering problem in the furnace allows the temperature of the flue gases to be kept as high as 1300 °C.

4.2. Feedstock

The coal feedstock conditions simulated are given in Table 4.

Table 4. Coal Feedstock Conditions for the Gasification Process.

Pittsburgh No. 8 Bituminous Coal	Mass Flow rate	19.44	kg/s
	Temperature	20	°C
	Particle Diameter	1.0	cm

Table 5 shows the proximate, ultimate and sulfur analyses of the feedstock coal, whose dry basis LHV is calculated as 32.32 MJ/kg using Boie Correlation with bias correction [29].

Table 5. Component Attributes of the Coal used in the Base case Model [9].

Proximate Analysis		Ultimate Analysis		Sulfur Analysis	
Element	**Value (wt. %)**	**Element**	**Value (wt. %, dry basis)**	**Element**	**Value (wt. %, dry basis)**
Moisture (wet basis)	4.58	C	77.76	Pyritic	0.87
		H	5.24	Sulfate	0.87
Fixed carbon (dry basis)	39.16	N	1.47	Organic	0.88
		Cl	0		
Volatile Matter (dry basis)	52.72	S	2.62		
		O	4.79		
Ash (dry basis)	8.12	Ash	8.12		

4.3. Terminologies

Conversion of coal, X_C, in the reactor is based upon the conversion of carbon content in the char introduced to the gasification process:

$$X_c = \frac{m_{C,in} - m_{C,out}}{m_{C,in}} \quad (9)$$

where;

$m_{C,in}$ = mass flow rate of elemental carbon of feed coal into the gasifier, kg/s.
$m_{C,out}$ = mass flow rate of elemental carbon in the solid outflow from the gasifier, kg/s.
Cold Gas Efficiency [10] of the process is calculated as:

$$Cold\ Gas\ Efficiency = \frac{LHV\ of\ Dry\ Syngas,\ \ MW}{LHV\ of\ Feed\ Coal,\ \ MW} \quad (10)$$

Syngas yield is defined as:

$$Syngas\ Yield = \frac{Mass\ flow\ rate\ of\ dry\ syngas, kg/sec}{Mass\ flow\ rate\ of\ coal\ feed, kg/sec} \quad (11)$$

"Condensate" is defined as the water removed from the raw syngas after condensation under pressure. This water must later be sent to the waste water treatment facility.

The two schemes developed in this paper simulate the production of syngas for a variety of purposes, not limited to power production. However, for the sake of comparison to conventional

gasification processes, a power generation scheme was also simulated which utilizes the products of Scheme1 and Scheme 2 to produce electricity through gas and steam turbines. The net electricity produced in the power generation schemes is then used to calculate thermal efficiency, defined as:

$$Thermal\ Efficiency\ = \frac{Electrical\ Power\ Produced - Auxiliary\ Power\ Requirement\ ,\ \ MW}{Coal\ Input\ Energy\ (LHV),\ \ MW} \quad (12)$$

4.4. Simultaneous Convergence of Energy Balances, Heat Integration and Reaction Kinetics

Three models are run iteratively in order to achieve a heat and temperature distribution which satisfies all of them in terms of conservation of energy and mass balances. These three models are:

1. Model for Reaction Kinetics (by Aspen Plus™)
2. Model for Process Simulation & Heat Integration (by Aspen Plus™)
3. Model for Heat Balance in bayonet heat exchangers (by MS Excel™)

For convergence, the iterations are locked when the following two conditions are fulfilled simultaneously:

$$\max_{i=1\ldots12}\left|T_{O,i,j} - T_{O,i,j-1}\right| < 0.8 \quad (13)$$

$$\max_{i=1\ldots12}\frac{\left|q_{i,j} - q_{i,j-1}\right|}{\sum_{i=1}^{12} q_{i,j}} \ < \ 0.06\% \quad (14)$$

Where,

$T_{O,i,j}$ = mean temperature of the gasifier gases across cell *i* in *j*th iteration, °C.

$q_{i,j}$ = heat transfer to the gasifier gases through cell *i* in *j*th iteration, MW.

Each one of the 12 bayonet cells corresponds to an RCSTR block unit in the Aspen Plus Simulation, as far as the heat transfer is concerned. The thermal and flow properties of the flue gases passing through the bayonet tube heat exchangers and the those of the mixture of steam and syngas flowing over the outer surface of the bayonets are retrieved from the Aspen Plus™ simulation and integrated in the MS Excel™ sheet. The volume flow rate over the bayonet surface and heat transfer of each cell is converged with the heat transfer taking place in the corresponding RCSTR unit. The Excel™ Solver tool is utilized to minimize the squared deviations of the heat balance equations (B1 - B7) listed in Appendix B.

Chart 1 depicts the flow of data for the convergence scheme among the three models.

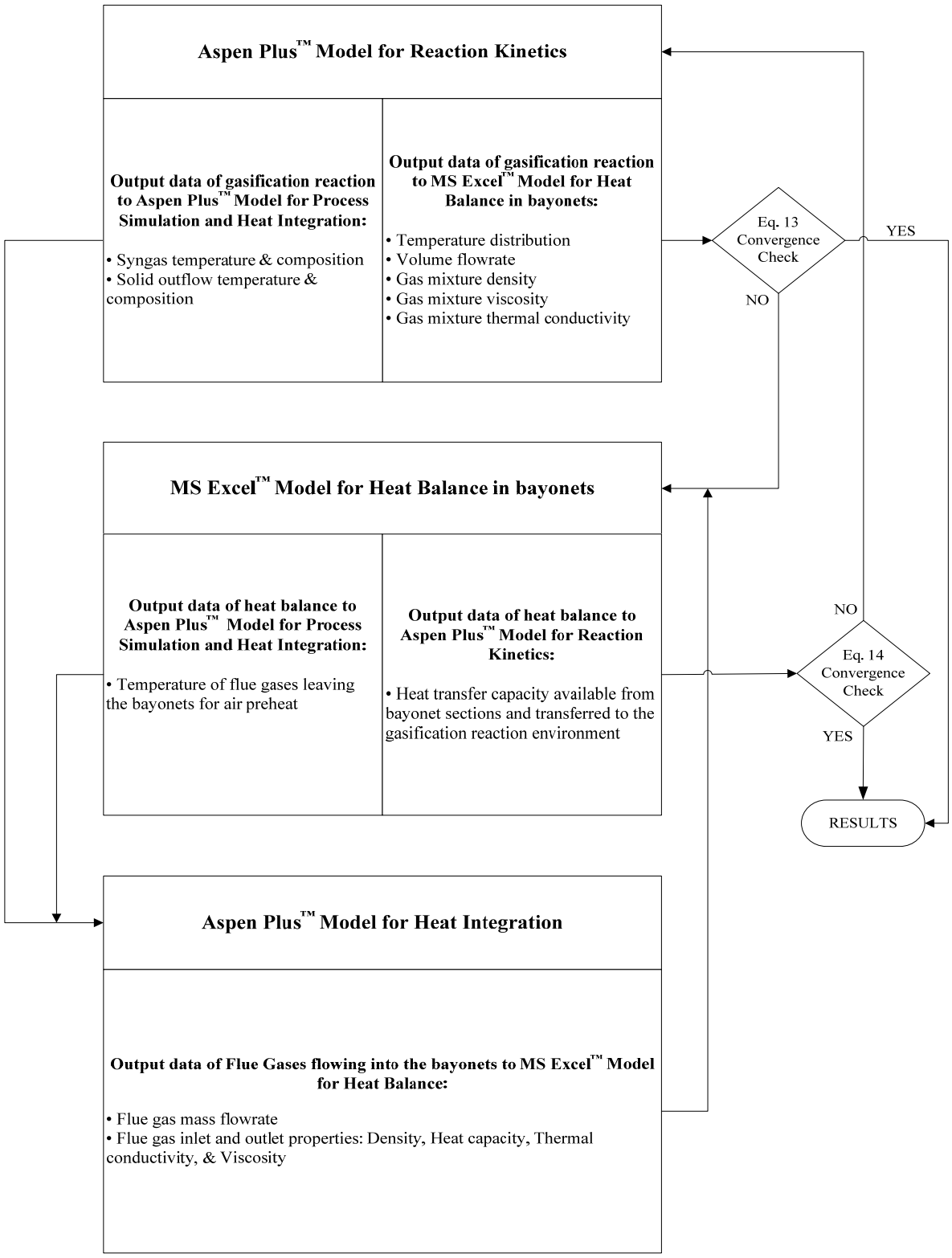

Chart 1. Scheme of inputs/outputs of each program used.

5. Results and Discussions

Simulation results for the two cases considered are presented in Table 6. The figures reported are based on the analysis of dry syngas after condensate removal from the raw syngas product stream.

Table 6. Simulation Results.

	Partial Syngas Combustion (Scheme 1)	Unreacted Char Combustion (Scheme 2)
Mass flow rate of syngas, dry basis (kg/s)	21.64	17.36
Molar flow rate of syngas, dry basis (kmol/s)	1.27	1.06
Mole% Composition (dry basis)		
CO	18.94%	12.53%
H_2	54.47%	50.97%
CO_2	17.67%	17.58%
CH_4	7.74%	16.24%
N_2	0.40%	0.91%
H_2S	0.21%	0.48%
C_6H_6	0.57%	1.29%
Mass flow rate of condensate (kg/s)	23.34	31.64
Condensate/Syngas, dry basis (kg/kg)	1.08	1.82
Conversion of C, in the gasifier (X_C)	95.52%	33.13%
H_2/CO Molar Ratio	2.88	4.07
Syngas Yield	1.11	0.89
Cold Gas Efficiency	59.85%	58.91%
LHV syngas, dry basis (MJ/kg)	16.58	20.42
LHV syngas, dry basis (MJ/kmol)	266.11	331.80
CO_2 produced per unit dry syngas (kmol/kmol)	0.589	0.766

Comparison of the two schemes analyzed, as presented in Table 6, shows that;

- In the unreacted char combustion case, the H_2/CO molar ratio is higher, because the higher steam flow rate and the lower gasification temperature favor the Water-Gas shift reaction.
- In the unreacted char combustion process, the conversion of coal in the gasifier is small, yet all of the residual carbon is combusted in the furnace for heat generation.100% of the coal heating value is utilized, contrary to the partial syngas combustion scheme where almost 4.48% of carbon in char remains unreacted.
- Due to lower temperature range of the unreacted char combustion process, the mole fraction of methane in the dry product gas is almost twice of that in the partial syngas combustion

process and in the conventional gasification process. Accordingly, a higher LHV of the syngas produced is obtained with the unreacted char combustion scheme.

- There is a lower flow rate of condensate in the partial product gas combustion scenario, as almost half of the raw syngas containing unreacted steam goes directly into the furnace for combustion, where it does not condense, but serves as a carrier of heat into the bayonet tubes. In the unreacted char scheme, this role is served by 10% more excess air in the furnace to provide optimum flow properties in the bayonets for the required heat transfer.

Table 7. Typical composition of the syngas (dry basis) obtained from Pittsburgh No. 8 Bituminous coal gasification in Lurgi Process [5].

Composition	Mole%
CO	16.9%
H_2	39.4%
CO_2	31.5%
CH_4	9.0%
H_2S	0.8%
N_2	1.6%
C_nH_m	0.8%
H_2/CO Molar Ratio	2.33
Cold Gas Efficiency	75.3%
Effective Efficiency	48.8%
LHV syngas, dry basis (MJ/kmol)	250.82
CO_2 produced per unit dry syngas (kmol/kmol)	0.665

In Table 7, some typical values of product composition for the gasification with oxygen are shown [5,9]. When comparing the dry basis molar compositions of syngas in Tables 6 and 7, it can be observed that in the steam gasification processes presently proposed, there is a higher molar composition of hydrogen or hydrogen containing compound (i.e. methane) and thus the carbon dioxide produced is considerably less. However, the carbon dioxide emissions from the processes here considered should take into account also the contributions of the flue gases (in our proposed schemes) and of the carbon dioxide produced in coal combustion to generate power for ASU and steam (in a Lurgi process). It should be observed that with respect to moles of dry syngas produced, the moles of CO_2 emitted collectively from the flue gases and the syngas product are the least in Scheme 1 as compared to the schemes with coal combustion i.e. the conventional Lurgi gasifier and the Scheme 2.

Further, the effective efficiency (defined as gross heating value of syngas produced per unit heating value of coal consumed in: gasification + generation of steam + power for the process) is higher for the presently proposed processes with respect to the Lurgi process if, in this last case, we take into account the energy required for the production of steam and power. For our schemes, the effective efficiency is practically represented by the cold gas efficiency.

Table 8 summarizes the results of the heat and temperature distribution in the bayonets and in the gasification reaction. Note that the total heat provided by the bayonets is only 24.93 MW in the case of unreacted char combustion as compared to 68.63 MW in the other case. Therefore, a lower heat duty and lower operating temperature range allow for a safer and more flexible operation and easier to fabricate construction materials.

Table 8. Results obtained from the heat balances for the base case.

	Partial Syngas Combustion	Unreacted Char Combustion
Total heat provided from the bayonets (MW)	68.63	24.93
Height of bayonets (m)	18.0	18.0
Temperature of Flue Gas exit from bayonets (°C)	1079.2	879.9
Range of Gasification temperature(°C)	926-1032	799-851
Heat Duty consumed in Drying and Pyrolysis(MW)	30.49	30.49
Temperature of Syngas + Steam at gasifier exit (°C)	661	504

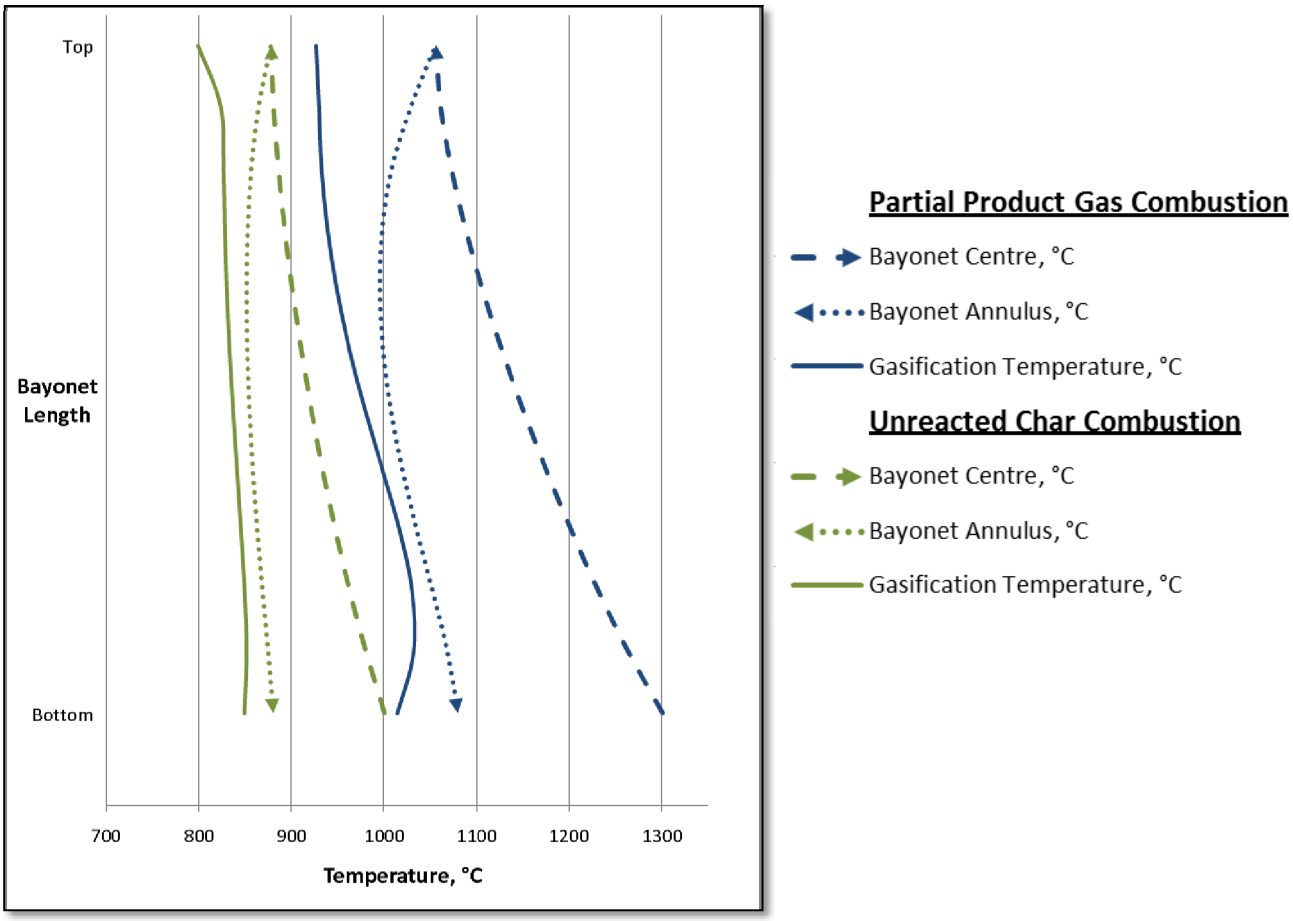

Figure 3. Temperature profiles along the length of bayonet heat exchangers.

In Figure 3, the temperature profiles of the flue gases are plotted in the two sections of the bayonet heat exchanger and of the syngas and steam mixture in the gasification reactor around the bayonets, for both Scheme 1 and Scheme 2. It is apparent that, in the partial product gas combustion scheme the overall temperature range is much larger. This fact might make the process safety and operational stability more challenging. There is a higher temperature gradient between the two temperature profiles in the bayonet sections, which justifies the use of the sintered α-SiC for bayonet core construction to withstand high temperature and an equally good and stable thermal conductivity to conduct the large heating power to be transferred.

The difference in the ranges of gasification temperatures between the two schemes is also visible in Figure 3. The unreacted char combustion scheme has a quite uniform temperature throughout the reactor height (overall $\Delta T = 52$ °C). This simplifies the equipment design as well as operation of the process.

Finally, to evaluate the thermal efficiency of the processes, a series of gas and steam turbines is arbitrarily simulated which utilizes the products (syngas and surplus steam) of the two proposed schemes and a Lurgi gasifier to produce power. The conventional process model is based on the one developed by Aspen to simulate the results presented by Wen et al. [5]. Oxygen to coal ratio is kept at 0.6 and the steam to coal ratio at 2.85 kg/kg [23]. Table 9 shows the breakdown of energy from input to output which allows calculating the final thermal efficiency.

Table 9. Comparison of Thermal Efficiencies for Gasification Schemes with Oxygen (Conventional), Partial Syngas Combustion, and Unreacted Char Combustion.

Energy, MW	Conventional O_2 Gasification	Partial Syngas Combustion (Scheme 1)	Unreacted Char Combustion (Scheme 2)
Coal Thermal Energy Input	609.5		
Syngas Thermal Energy Content	500	646.4	353
Thermal Energy Drainage: - **Steam Generation** - **Indirect Gasification Heat**	 166.3* 0	 293.2 68.6	 0 0
Gross Power Produced	301.1	216.7	188.1
Electrical Energy Drainage: - **Air Separation Unit**	16.9*	0	0
Auxiliary Power Consumption (2.5% of gross power generation)†	7.5	5.4	4.7
Net Electrical Power	276.7	211.3	183.4
Thermal Efficiency	45.40%	34.67%	30.09%

* *These values are calculated as indicated by Higman and Van der Burgt* [7].

† *These values are calculated on the basis of values provided by Zheng and Furinsky* [30].

The syngas energy content for Scheme 1 seems higher than the energy coming in with coal but it should be noted that this gasification process takes energy input from coal as well as from the incoming steam and the bayonets. Thus, when the flue gases are generated from the combustion of a part of the syngas produced to cater for these heat provisions, there is an effect on the net power produced. Energy required for steam is taken from the hot flue gases generated by the combustion of syngas. Therefore, for the scheme 2, this value remains zero as the steam is generated by the combustion of unreacted char, not the syngas. Similarly, the gasification heat input is also zero for the Scheme 2 as the flue gases for this purpose are also from unreacted char combustion rather than syngas. For a conventional process, there is no indirect heat provision. The gross power produced includes power obtained from the use of net syngas output and surplus steam in a gas and steam turbine combined cycle plant. After deducting power required for air separation unit and auxiliaries (where applicable), the net power produced in each scheme is listed to finally calculate the thermal efficiency as per Eq. 12.

For the given type of coal and the gasifier configuration, the above comparison shows that the schemes proposed in this paper have lower thermal efficiencies as compared to the conventional gasification with oxygen; therefore they are less suitable for power generation purposes. However, in the case of chemical synthesis, our schemes offer the advantage of avoiding the need of energy consumption in an air separation unit and lower carbon dioxide content in the product gas.

6. Conclusions

In this paper, a gasification process using solely high temperature and high pressure steam as a gasifying medium has been developed, simulated and analyzed. The heat for endothermic reaction is indirectly provided through bayonet tube heat exchangers installed inside the gasifier, through which hot flue gases from hydrocarbon combustion are passed. To generate these, part of the raw syngas produced (Scheme 1) or the unreacted char from partial conversion in gasification (Scheme 2) are used. Both of these two schemes are optimized for heat integration and simulated to achieve energetically self-sufficient processes.

The cold gas efficiencies for the two proposed schemes are very close and also represent the effective efficiencies of the schemes which remain higher as compared to a typical Lurgi gasifier with air separation unit. Though the gasification process with partial syngas combustion has a H_2/CO ratio much closer to conventional gasification processes (which makes the product more suitable for downstream applications), in terms of the lower heating value, the gasification scheme with unreacted char combustion gives better results as it operates at lower gasification temperature, giving higher H_2/CO ratio and a higher content of methane. It also requires less temperature gradient for heat transfer (i.e. it does not require the use of special materials).

The thermal efficiencies for the proposed schemes are much less than typical BGL gasifier (typically more than 40% [30]), therefore, keeping in view the elimination of the requirement of an Air Separation Unit and lower molar content of carbon dioxide in product gas, these schemes might be suggested for syngas production for refinery utilities, chemical synthesis, and SNG and liquid fuels production rather than for power production. Table 10 provides a qualitative comparison of the schemes as discussed above.

The proposed process schemes are highly integrated and a careful formulation of their start-up, shutdown, and control procedures is of utmost importance. Moreover the construction of such types of bayonet heat exchanger banks and their mechanical integration to the gasifier body poses a major challenge for the realization of such scheme. This asks for further extensive studies of these proposed schemes from the mechanical, constructional, operational and economical aspects.

Table 10. Qualitative Comparison of Gasification Schemes: Conventional (with Oxygen), Partial Syngas Combustion, and Unreacted Char Combustion.

	Conventional O_2 Gasification	Partial Syngas Combustion	Unreacted Char Combustion
Cold Gas Efficiency	↑	↓	↓
Effective Efficiency	↓	↑	↑
Thermal Efficiency	↑	↔	↓
LHV, dry basis	↓	↔	↑
H_2/CO ratio	↔	↔	↑
Molar CO_2 Content	↑	↓	↓
Syngas Yield	↑	↔	↓
Overall CO_2 Emission	↔	↓	↑

↓ **Low** ↔ **Medium / Equivalent** ↑ **High**

APPENDIX A

Rate Equation for Reaction (2):

The rate equation of the reaction (2) with respect to oxygen, R_{C-O_2} (mol/cm^3.s), is based on the unreacted-shrinking core model [9, 31]:

$$R_{C-O_2} = \frac{P_{O_2}}{\frac{1}{k_{film}} + \frac{1}{k_s Y^2} + \frac{1}{k_{dash}}} \qquad \text{(A1)}$$

where,

k_{film} = gas film diffusion constant, mol/cm^3.atm.s.

k_s = chemical reaction constant, mol/cm^3.atm.s.

k_{dash} = ash diffusion coefficient, mol/cm^3.atm.s.

P_{O_2} = partial pressure of oxygen, atm.

$$Y = \frac{r_{core}}{r_{particle}} = \left(\frac{1-x}{1-f}\right)^{\frac{1}{3}} \qquad \text{(A2)}$$

with,

r_{core} = radius of unreacted core, cm.

$r_{particle}$ = radius of feed coal particle, cm.

x = coal conversion at any time after pyrolysis is completed, based on dry-coal.

f = coal conversion when pyrolysis is completed, based on dry-coal.

The particle size of the coal fed to the moving bed gasifier is taken as 1 cm.

Since reaction (2) is a surface reaction and k_s value is high when compared to k_{film} and k_{dash}, equation (8) can be simplified to:

$$R_{C-O_2} = \frac{P_{O_2}}{\frac{1}{k_{film}} + \frac{1}{k_{dash}}} \quad \text{(A3)}$$

where,

$$k_{film} = 0.292 \text{ x } 4.26 \text{ x } \frac{\left(\frac{T}{1800}\right)^{1.75}}{d_p T}$$

$$k_{ash} = k_{film} . \varepsilon_p^{2.5} . \frac{Y}{1-Y}$$

d_p = diameter of feed coal particle, cm.

ε_p = porosity of ash, dimensionless. In the model, ε_p= 0.75 [23]

Rate Equation for Reaction (3) [9]:

Reaction rate between carbon and water, R_{C-H_2O} (mol/cm^3.s.);

$$R_{C-H_2O} = 930 e^{\frac{-45000}{1.987\,T}} . C_C . (P_{H_2O} - P^*_{H_2O}) \quad \text{(A4)}$$

where,

C_C=Concentration of carbon, mol/cm^3.

P_{H_2O}=Partial pressure of steam in the reactor, atm.

$P^*_{H_2O} = \frac{P_{H_2} . P_{CO}}{e^{17.29 - \frac{16330}{T}}}$, atm.

P_{H_2}=Partial pressure of hydrogen in the reactor, atm.

P_{CO}=Partial pressure of carbon-monoxide in the reactor, atm.

Rate Equation for Reaction (4) [9]:

Reaction rate between carbon and carbon-dioxide, R_{C-CO_2}(mol/cm^3.s.);

$$R_{C-CO_2} = 930 e^{\frac{-45000}{1.987\,T}} . C_C . (P_{CO_2} - P^*_{CO_2}) \quad \text{(A5)}$$

where,

P_{CO_2}=Partial pressure of carbon-dioxide in the reactor, atm.

$P^*_{CO_2} = \frac{P^2_{CO}}{e^{20.92 - \frac{20280}{T}}}$, atm.

Rate Equation for Reaction (5) [9]:

Reaction rate between carbon and hydrogen, R_{C-H_2}, (mol/cm^3.s.);

$$R_{C-H_2} = e^{-7.087-\frac{8078}{T}}.C_C.(P_{H_2} - P^*_{H_2}) \qquad \text{(A6)}$$

where,

$$P^*_{H_2} = \left(\frac{P_{CH_4}}{e^{-13.43+\frac{10100}{T}}}\right)^{0.5}, \text{atm} \qquad \text{(A7)}$$

P_{CH_4}=Partial pressure of methane in the reactor, atm.

Rate Equation for Reaction (6) [9]:

Reaction rate for water-gas shift reaction, R_{CO-H_2O}, (mol/s.g. of ash.), is based on the reactors which mostly employ an iron-based catalyst to produce hydrogen from CO and H_2O. Since, in the simulation, no such catalyst is employed, yet ash in its reactivity serves as a catalyst in the water-gas shift reaction, a correction factor is assumed, representing the reactivity of ash in the char as a catalyst. Therefore we have,

$$R_{CO-H_2O} = F_w \text{ x } 2.877 \text{ x } 10^5.e^{-\frac{27760}{1.987T}}.\left(x_{CO}.x_{H_2O} - \frac{x_{CO_2}.x_{H_2}}{k_{wgs}}\right).P_t^{0.5-\frac{P_t}{250}}.e^{-8.91+\frac{5553}{T}} \qquad \text{(A8)}$$

where,

F_w=Correction factor taking into account the relative reactivity of ash to the iron-base catalyst, dimensionless. In the model, F_w=0.0084 [24].

x_{CO}=Mole fraction of carbon-monoxide in the reactor, dimensionless.

x_{H_2O}=Molar Fraction of steam in the reactor, dimensionless.

$$P^*_{H_2O} = \frac{P_{H_2}.P_{CO}}{e^{17.29-\frac{16330}{T}}}, \text{atm} \qquad \text{(A9)}$$

x_{CO_2}=Mole fraction of carbon-dioxide in the reactor, dimensionless.

x_{H_2}=Molar Fraction of hydrogen in the reactor, dimensionless.

Water Gas shift rate constant, $k_{wgs} = e^{-3.6890+\frac{7234}{1.8T}}$ (A10)

P_t=Total pressure, atm.

Rate Equation for Reaction (7) [32]:

Reaction rate between hydrogen and oxygen, $R_{H_2-O_2}$, (mol/m^3.s.);

$$R_{H_2-O_2} = 8.83 \text{ x } 10^5.e^{-\frac{9.976 \text{ x } 10^4}{8.315\,T}}.C_{H_2}.C_{O_2} \qquad \text{(A11)}$$

where,

C_{H_2}= Concentration of hydrogen, mol/m^3.

C_{O_2}= Concentration of oxygen, mol/m^3.

APPENDIX B

Following energy balance equations are formulated for the conduction, convection and radiation heat transfers among different sections of any given cell *'i'* of the bayonet tube.

Bayonet center pipe to inner wall:

$$2\pi R_1 \Delta z h_{1,i}\left(T_{C,i} - T_{1,i}\right) = \frac{2\pi \Delta z k_I}{\ln\frac{R_2}{R_1}}\left(T_{1,i} - T_{2,i}\right) \quad \text{(B1)}$$

Convection of hot flue gas along inside centre pipe wall — Conduction through centre pipe wall

where,

R_1 = Internal radius of the bayonet inner tube (core), m.

R_2 = External radius of the bayonet inner tube (core), m.

Δz = Height of one bayonet tube cell = 1.50 m.

$h_{1,i}$ = Heat transfer coefficient of the flue gas flowing through the inner tube, W/m^2.K.

k_I = Thermal Conductivity of the core material, W/m.K.

$T_{C,i}$ = Temperature of gas in the bayonet inner tube, K.

$T_{1,i}$ = Core inner wall temperature, K.

$T_{2,i}$ = Core outer wall temperature, K.

Bayonet center pipe outer wall to annulus:

$$\frac{2\pi \Delta z k_I}{\ln\frac{R_2}{R_1}}\left(T_{1,i} - T_{2,i}\right) = 2\pi R_2 \Delta z h_{2,i}\left(T_{2,i} - T_{A,i}\right) + 2\pi R_2 \Delta z \sigma \varepsilon \left[\left(T_{2,i}\right)^4 - \left(T_{3,i}\right)^4\right] \quad \text{(B2)}$$

Conduction through centre pipe wall — Convection of hot flue gas along outside centre pipe wall — Radiation from centre pipe wall to the annulus inner wall

where,

$h_{2,i}$ = Heat transfer coefficient of the flue gas flowing through the annular section adjacent to the center pipe outer wall, W/m^2.K.

$T_{A,i}$ = Temperature of gas in the annular section, K.

σ = Stefan-Boltzmann constant = 5.6688 x 10^{-8} W/m^2.K.

ε = Effective emissivity for infinitely grey, concentric cylinders.

$$= \frac{1}{\frac{1}{\varepsilon_2} + \frac{R_2}{R_3}\left(\frac{1}{\varepsilon_3} - 1\right)}$$

ε_2 = Surface Emissivity of the inner tube.

ε_3 = Surface Emissivity of the metallic outer shell.

$T_{3,i}$ = Annulus inner wall temperature, K.

Annulus to metallic inner wall:

$$2\pi R_3 \Delta z h_{3,i}\left(T_{A,i} - T_{3,i}\right) + \ 2\pi R_2 \Delta z \sigma \varepsilon \left[\left(T_{2,i}\right)^4 - \left(T_{3,i}\right)^4\right] \ = \ \frac{2\pi \Delta z k_O}{\ln\frac{R_4}{R_3}}\left(T_{3,i} - T_{4,i}\right) \quad \text{(B3)}$$

Conduction through annulus pipe wall | Radiation from center pipe wall to the annulus inner wall | Convection of hot flue gas along inside annulus wall

where,

$h_{3,i}$ = Heat transfer coefficient of the flue gas flowing through the annular section adjacent to the annulus inner wall, W/m^2.K.

k_O = Thermal Conductivity of the annulus material, W/m.K.

R_3 = Internal radius of the annulus, m.

R_4 = External radius of the annulus, m.

$T_{4,i}$ = Annulus outer wall temperature, K.

Annulus pipe outer wall to gasifier environment:

$$\frac{2\pi \Delta z k_O}{\ln\frac{R_4}{R_3}}\left(T_{3,i} - T_{4,i}\right) \ = \ 2\pi R_4 \Delta z h_{4,i}\left(T_{4,i} - T_{O,i}\right) + \ 2\pi R_4 \Delta z \sigma C_r \left[\left(T_{4,i}\right)^4 - \left(T_{O,i}\right)^4\right] \text{(B4)}$$

Conduction through annulus pipe wall | Convection of steam + syngas along outside annulus wall | Radiation from annulus wall to the gasifier environment

where,

$h_{4,i}$ = Heat transfer coefficient of the steam + syngas mixture flowing over the outer annular wall, W/m^2.K.

$T_{O,i}$ = Temperature of mixture of gases in the gasifier, K.

C_r = Radiation constant = 1 [27]

Net Heat Provided

$$\frac{2\pi \Delta z k_O}{\ln\frac{R_4}{R_3}}\left(T_{3,i} - T_{4,i}\right) \ = \ q_i \quad \text{(B5)}$$

Conduction through annulus pipe wall | Heat provided for gasification by cell *'i'* of a tube, W/tube

Energy Balance between two adjacent cells

An energy balance is required between the two adjacent cells *'i'* and *'i+1'* both in the center pipe and in the annular section.

$$\dot{m} C_{p,i} T_{C,i} = \ \dot{m} C_{p,i+1} T_{C,i+1} + 2\pi R_1 \Delta z h_1 \left(\overline{T_{C,i}} - \overline{T_{1,i}}\right) \quad \text{(B6)}$$

where,

$\dot{m}$ = Mass flowrate of flue gases, kg/s.

C_p = Specific heat of the flue gas, J/kg.K.

$$h_1 = \frac{1}{2}(h_{1,i} + h_{1,i+1})$$

$$\overline{T_{C,\iota}} = \frac{1}{2}(T_{C,i} + T_{C,i+1})$$

$$\overline{T_{1,\iota}} = \frac{1}{2}(T_{1,i} + T_{1,i+1})$$

And,

$$\dot{m}C_{p,i}T_{A,i} + 2\pi R_3 \Delta z h_3\left(\overline{T_{A,\iota}} - \overline{T_{3,\iota}}\right) = \dot{m}C_{p,i+1}T_{A,i+1} + 2\pi R_2 \Delta z h_2(\overline{T_{2,\iota}} - \overline{T_{A,\iota}}) \quad \text{(B7)}$$

where,

$$h_2 = \frac{1}{2}(h_{2,i} + h_{2,i+1})$$

$$h_3 = \frac{1}{2}(h_{3,i} + h_{3,i+1})$$

$$\overline{T_{A,\iota}} = \frac{1}{2}(T_{A,i} + T_{A,i+1})$$

$$\overline{T_{2,\iota}} = \frac{1}{2}(T_{2,i} + T_{2,i+1})$$

$$\overline{T_{3,\iota}} = \frac{1}{2}(T_{3,i} + T_{3,i+1})$$

Heat Transfer Coefficient

$$h_{\mathrm{i}} = \frac{k_{\mathrm{i}} Nu_{\mathrm{i}}}{2\mathrm{R_i}} \quad \text{(B8)}$$

where,

Nu_i = Nusselt Number in/over cell i,

h_i= Heat Transfer Co-efficient in/over cell i, W/m^2.K.

k_i = Thermal conductivity of flue gases in/mixture of gasifier gases over cell i, W/m.K.

R_i = Radius (with respect to the related geometry) of cell i, m.

Nusselt Number

In the center pipe, Dittus & Boelter [33] recommend following expression for fully developed heat releasing turbulent flow in smooth pipes,

$$\mathrm{Nu_C} = 0.023\ \mathrm{Re_C^{0.8}Pr_C}^{0.33} \quad \text{(B9)}$$

where,

Nu_c = Nusselt Number in the center pipe of bayonet,

Re_c = Reynolds number in the center pipe of bayonet,

Pr_c = Prandtl number in the center pipe of bayonet.

With a fully developed turbulent flow in a smooth annular section between two concentric pipes, following expression, suggested by Incropera and Dewitt [34] can be used.

$$\mathrm{Nu_A} = 0.02\ \mathrm{Re_A^{0.8}Pr_A}^{0.333}\left(\frac{\mathrm{R_3}}{\mathrm{R_2}}\right)^{0.53} \quad \text{(B10)}$$

where,

Nu_A = Nusselt Number in the annular section of bayonet,

Re_A = Reynolds number in the annular section of bayonet,

Pr_A = Prandtl number in the annular section of bayonet.

In an experimental study of a cylinder in axial flow, mentioned by Wiberg and Lior [35], Nusselt number was correlated as follows, for the axial flow of gasifier gases over cylindrical surfaces.

$$\mathrm{Nu_O} = 0.927\ \mathrm{Re_O^{0.5}} \quad \text{(B11)}$$

where,

Nu_O = Nusselt Number of the gasifier gases flowing over the bayonet pipe,

Re_O = Reynolds number of the gasifier gases flowing over the bayonet pipe.

Reynolds Number

In the center pipe, Reynolds Number is calculated as,

$$\mathrm{Re_C} = \frac{\mathrm{U_C 2R_1}}{\upsilon_\mathrm{C}} \quad \text{(B12)}$$

where,

U_C = Average velocity of flue gases in center pipe, m/s.

υ_C = Kinematic Viscosity of flue gases in center pipe, m^2/s.

In the annulus, Reynolds number of the flue gases is calculated as,

$$\mathrm{Re_A} = \frac{\mathrm{U_A 2R_{eq}}}{\upsilon_\mathrm{A}} \quad \text{(B13)}$$

where,

U_A = Average velocity of flue gases in annulus, m/s.

υ_A = Kinematic Viscosity of flue gases in annulus, m^2/s.

R_{eq} = Equivalent Radius of the annular portion, m.

$$\mathrm{R_{eq}} = \frac{2(R_3^2 - R_2^2)}{R_2} \quad \text{(B14)}$$

For the flow of mixture of gases over the bayonet tubes in the gasifier environment, the Reynolds number is calculated as follows,

$$Re_O = \frac{V_O D_H}{\upsilon_O(1-\epsilon)} \quad \text{(B15)}$$

where,

V_O = Superficial velocity of gasifier gases per tube, m/s.

D_H = Gasifier Hydraulic Diameter, m.

$$\mathrm{D}_H = \frac{4\,A_x}{WP} \quad \text{(B16)}$$

A_x = Total cross-sectional area of the gasifier, m^2.

WP = Wetted Perimeter by the flow of gasifier gases, m.

= Inner Circumference of Gasifier + 487 x Outer Circumference of a bayonet tube

υ_O = Kinematic Viscosity of gasifier gases, m^2/s.

ϵ = Bed Voidage, varying from 0.4 to 0.7 for each cell.

Prandtl Number

Prandtl number of the flue gases in each cell of the center pipe and the annulus and that of the mixture of Syngas and steam in the Gasifier environment is calculated as,

$$Pr = \frac{C_P \mu}{k} \qquad \text{(B17)}$$

where,

k= Thermal conductivity of flue gases, W/m.K.

μ= Dynamic Viscosity of flue gases, Pa.s.

APPENDIX C

The materials of construction for bayonet core and annular tubes are selected on the basis of temperatures observed in the simulation. The properties listed below are used in the heat balance equations for the bayonet heat exchangers given in Appendix B.

HK-40 Heat Resistant Alloy:

Service Temperature: 1093°C [37]

Thermal Conductivity: $0.000007\ T^2 + 0.0088\ T + 14.164$, W/m.K (C1)

where,

T = Wall Temperature (871°C to 1093°C) [37-38]

Emissivity: 0.97

Emissivity of HK-40 alloy is estimated to be equivalent to that of oxidized 20-Ni,24-Cr alloy [39] which has the most comparable composition with HK-40.

Sintered α-SiC Ceramic:

Service Temperature: 1600°C [40]

Thermal Conductivity: $\frac{52000\ e^{-1.24\ .10^{-5}.T}}{T+437}$ (C2)

where,

T = Wall Temperature (0°C to 2000°C), [36]

Emissivity: 0.96

Emissivity of SiC ceramic increases from 0.83 to 0.96 over temperature range of 149°C to 649°C [41]. In this work, the value of 0.96 is used for higher temperatures as well.

Acknowledgements

This study has been performed with the financial support from Erasmus Mundus EMMA-WEST Action 2 program.

Conflict of Interest

The authors declare no conflict of interest.

References

1. Lucquiaud M, Gibbins J (2011) On the integration of CO_2 capture with coal-fired power plants: a methodology to assess and optimise solvent-based post-combustion capture systems. *Chem Eng Res Des* 89: 1553–1571.
2. EU Commission (2006) Commission communication on sustainable power generation from fossil fuels: aiming from near zero emissions from coal after 2020. Summary of the impact assessment. *SEC* 1723.
3. Engelbrecht AD, North BC, Oboirien BO (2010) Making the most of South Africa's low-quality coal: Converting high-ash coal to fuel gas using bubbling fluidised bed gasifiers. In: CSIR, Science Real and Relevant Conference, Pretoria (South Africa), EN06-PA-F.
4. Sudiro M, Pellizzaro M, Bezzo F, et al. (2010b) Simulated moving bed technology applied to coal gasification. *Chem Eng Res Des* 88: 465–475.
5. Wen CY, Desai PR, Lin CY (1975) Factors Affecting the Thermal Efficiency of a Gasification Process. *Chem Soc Div Fuel Chem Prepr* 20: 219–226.
6. Majoumerd MM, Raas H, De S, et al. (2014) Estimation of performance variation of future generation IGCC with coal quality and gasification process—Simulation results of EU H2-IGCC project. *Appl Energy* 113: 452–462.
7. Higman C, Van der Burgt M (2008) Gasification. Gulf Professional Publishing, Elsevier Science (USA).
8. Bayarsaikhan B, Sonoyama N, Hosokai S, et al. (2006) Inhibition of steam gasification of char by volatiles in a fluidized bed under continuous feeding of a brown coal. *Fuel* 85: 340–349.
9. Wen CY, Chen H, Onozaki M (1982) User's Manual for Computer Simulation and Design of the Moving Bed Coal Gasifier. DOE/MC/16474-1390.
10. Sudiro M, Bertucco A, Ruggeri F, et al. (2008) Improving Process Performances in Coal Gasification for Power and Synfuel Production. *Energy Fuels* 22: 3894–3901.
11. Sudiro M, Zanella C, Bertucco A, et al. (2010a) Dual-Bed Gasification of Petcoke: Model Development and Validation. *Energy Fuels* 24: 1213–1221.
12. Zhang Y, Wang Y, Cai L, et al. (2013) Dual bed pyrolysis gasification of coal: Process analysis and pilot test. *Fuel* 112: 624–634.
13. Arthur CJ, Munir MT, Young BR, et al. (2014) Process simulation of the transport gasifier. *Fuel* 115: 479–489.

14. Feng X, He C, Chu KH (2013) Process modeling and thermodynamic analysis of Lurgi fixed-bed coal gasifier in an SNG plant. *Appl Energy* 111: 742–757.
15. Kawabata M, Kurata O, Iki N, et al. (2012) Advanced integrated gasification combined cycle (A-IGCC) by exergy recuperation—technical challenges for future generations. *J Power Tech* 92: 90–100.
16. Duan W, Yu Q, Xie H, et al. (2014) Thermodynamic analysis of hydrogen-rich gas generation from coal/steam gasification using blast furnace slag as heat carrier. *Int J Hydrogen Energy* 39: 11611–11619.
17. O'Doherty T, Jolly AJ, Bates CJ (2001) Analysis of a bayonet tube heat exchanger. *Appl Therm Eng* 21: 1–18.
18. McKetta JJ (1992) Heat Transfer Design Methods. New York (USA): M. Dekker.
19. Hobbs ML, Radulovic PT, Smoot LD (1992) Modeling fixed-bed coal gasifiers. *AIChE J* 38: 681–702.
20. Larson ED, Jin H, Celik F (2004) Production of Electricity and/or Fuels from Biomass by Thermochemical Conversion. In: RBAEF Meeting, Washington, D.C. (USA).
21. Luberti M, Friedrich D, Ozcan DC, et al. (2014) Cogeneration of ultrapure hydrogen and power at an advanced integrated gasification combined cycle with pre-combustion capture. In: The 12th IChemE European Gasification Conference: New Horizons in Gasification, Rotterdam (Netherlands).
22. Benson SA, Sondreal EA, Hurley JP (1995) Status of coal ash behavior research. *Fuel Process Technol* 44: 1–12.
23. Aspen Plus (2012) Model for Moving Bed Coal Gasifier, v8.0. Berlington, USA.
24. Suuberg EM, Peters WA, Howard JB (1978) Product composition and kinetics of lignite pyrolysis. *Ind Eng Chem Process Des Dev* 17: 37–46.
25. Rinard IH, Benjamin BW (1985) Great plains ASPEN model development: gasifier model. *Literature Review and Model Specification*. DOE/MC/19163-1782.
26. Wen CY, Chaung TZ (1979) Entrainment coal gasification modelling. *Ind Eng Chem Process Des Dev* 18: 684–695.
27. Bussman W, Baukal C, French K. Variable Test Furnace Cooling. 2005 Summer Heat Transfer Conference, San Francisco (USA). HT2005-72012.
28. Foster Wheeler Italiana S.p.a., 2013, Personal communication.
29. Institute of Gas Technology (1976) Coal Conversion Systems Technical Data Book, Section PMa. 44.1.
30. Zheng L, Furinsky E (2005) Comparison of Shell, Texaco, BGL and KRW gasifiers as part of IGCC plant computer simulations. *Energ Convers Manage* 46: 1767–1779.
31. Kunii D, Levenspiel O (1991) Fluidization engineering. 2nd edition. Boston, USA: Butterworth-Heinemann.
32. Cen KF, Ni MJ, Luo ZY, et al. (1998) Theory, design and operation of circulating fluidized bed boilers. Chinese Electric Power Press, Beijing (China).
33. Dittus FW, Boelter LMK (1930) Heat Transfer in Turbulent Pipe and Channel Flow. Publications on Engineering, University of California, Berkeley 2: 443–461.

34. Incropera FP; Dewitt DP (2001) Fundamentals of Heat and Mass Transfer. New York, USA: Wiley.
35. Wiberg R, Lior N (2005) Heat transfer from a cylinder in axial turbulent flows. *Int J Heat Mass Transfer* 48: 1505–1517.
36. Munro RG (1997) Material Properties of a Sintered α-SiC. Ceramics Division, National Institute of Standards and Technology, Gaithersburg, Maryland 20899, USA.
37. Kubota Metal Corporation. Available from: http://www.kubotametal.com/alloys/heat_resistant/hk-40.pdf (accessed 26-Jun-2014).
38. NiPERA (Nickel Producers Environmental Research Association) (1974) Cast heat-resistant alloys. Available from: http://www.nipera.org/~/Media/Files/TechnicalLiterature/CastHeat_ResistantAlloys_ 1196_.pdf (accessed 28-Nov-2014).
39. Emissivity of Common Materials. Available from: http://www.omega.com/literature/transactions/volume1/emissivitya.html (accessed 26-Jun-2014).
40. http://www.sentrotech.com/shop/silicon-carbide-tubes-6978 (accessed 26-Jun-2014).
41. Emissivity of Common Materials. Available from: http://www.omega.com/literature/transactions/volume1/emissivityb.html (accessed 26-Jun-2014).

AIMS Press